J. Phycol. **48,** 559–568 (2012)

DOI: 10.1111/j.1529-8817.2012.01148.x

MORPHOLOGICAL AND PHYSIOLOGICAL EFFECTS IN *PROBOSCIA ALATA* (BACILLARIOPHYCEAE) GROWN UNDER DIFFERENT LIGHT AND CO_2 CONDITIONS OF THE MODERN SOUTHERN OCEAN[1]

Astrid Hoogstraten,[2] *Klaas R. Timmermans*

Department of Biological Oceanography, NIOZ Royal Netherlands Institute for Sea Research, PO Box 59, 1790 AB Den Burg, The Netherlands

and Hein J. W. de Baar

Department of Ocean Ecosystems, University of Groningen, Nijenborgh 7, 9747 AG Groningen, The Netherlands

The combined effects of different light and aqueous CO_2 conditions were assessed for the Southern Ocean diatom *Proboscia alata* (Brightwell) Sundström in laboratory experiments. Selected culture conditions (light and $CO_{2(aq)}$) were representative for the natural ranges in the modern Southern Ocean. Light conditions were 40 (low) and 240 (high) µmol photons $\cdot m^{-2} \cdot s^{-1}$. The three $CO_{2(aq)}$ conditions ranged from 8 to 34 µmol $\cdot kg^{-1}$ $CO_{2(aq)}$ (equivalent to a pCO_2 from 137 to 598 µatm, respectively). Clear morphological changes were induced by these different $CO_{2(aq)}$ conditions. Cells in low [$CO_{2(aq)}$] formed spirals, while many cells in high [$CO_{2(aq)}$] disintegrated. Cell size and volume were significantly affected by the different $CO_{2(aq)}$ concentrations. Increasing $CO_{2(aq)}$ concentrations led to an increase in particulate organic carbon concentrations per cell in the high light cultures, with exactly the opposite happening in the low light cultures. However, other parameters measured were not influenced by the range of $CO_{2(aq)}$ treatments. This included growth rates, chlorophyll *a* concentration and photosynthetic yield (F_V/F_M). Different light treatments had a large effect on nutrient uptake. High light conditions caused an increased nutrient uptake rate compared to cells grown in low light conditions. Light and CO_2 conditions co-determined in various ways the response of *P. alata* to changing environmental conditions. Overall *P. alata* appeared to be well adapted to the natural variability in light availability and $CO_{2(aq)}$ concentration of the modern Southern Ocean. Nevertheless, our results showed that *P. alata* is susceptible to future changes in inorganic carbon concentrations in the Southern Ocean.

Key index words: Proboscia alata; **culture experiments; irradiance; physiology; aqueous CO_2; dissolved inorganic carbon; total alkalinity**

Abbreviations: **DIC, dissolved inorganic carbon; A_T, total alkalinity; HL, high light; LL, low light; aq, aqueous; NIOZ, Royal Netherlands Institute for Sea Research; F_0, chlorophyll *a* autofluorescence; F_M, maximum chlorophyll *a* fluorescence; F_V/F_M, photochemical quantum efficiency; DOC, dissolved organic carbon (µmol $\cdot L^{-1}$); TOC, total organic carbon (µmol $\cdot L^{-1}$); POC, particulate organic carbon (µmol $\cdot$ cell^{-1}); PON, particulate organic nitrogen (µmol $\cdot$ cell^{-1}); CO_2, carbon dioxide; $CO_{2(aq)}$, aqueous carbon dioxide; $CO_{2(g)}$, gaseous carbon dioxide; HCO_3^-, bicarbonate ion; CO_3^{2-}, carbonate ion; pCO_2, partial pressure of CO_2; PAR, photosynthetically active radiation**

The Southern Ocean is characterised by strong vertical mixing and seasonality of solar irradiance, ice cover, and cloud cover. This causes a wide range in availability of Photosynthetically Active Radiation (PAR, 400–700 nm) at the sea surface and throughout the euphotic zone. High variability in light availability, ranging between 0 and 800 µmol $\cdot$ photons$\cdot m^{-2} \cdot s^{-1}$ in late summer, has proven to be the major limitation to phytoplankton growth in the Southern Ocean, in combination with the general deficiency of trace nutrient iron (Fe) in open ocean regions of the Southern Ocean (Mitchell et al. 1991, De Baar et al. 2005 and references therein, Alderkamp et al. 2010, 2011). Several studies have shown that more favourable light conditions increase growth rates of Southern Ocean phytoplankton, even with low iron availability (Boyd et al. 2001, Timmermans et al. 2001).

Favourable light conditions and adequate Fe supply, notably in near shore regions, may lead to occasions of intense photosynthesis and major CO_2 depletion in phytoplankton blooms, resulting in very low CO_2 conditions. On the other hand, unfavourable light and Fe conditions in combination with regimes of upwelling CO_2-rich deep water result in quite high ambient CO_2 conditions, since deep waters are rich in CO_2 due to respiration and mineralization. As a result there is a large range of

[1]Received 23 December 2010. Accepted 26 January 2012.
[2]Author for correspondence: e-mail astrid.hoogstraten@nioz.nl.

ambient concentrations of aqueous CO_2 ($CO_{2(aq)}$) in the modern Southern Ocean.

Most often the $CO_{2(aq)}$ in surface waters is quantified indirectly by the measurement of the partial pressure of gaseous CO_2 ($CO_{2(g)}$) in the seawater (the apparent pCO_2 of the surface waters). The natural range of pCO_2 reported ranges from as low as about 100 μatm in spring bloom waters in the Ross Sea (Sweeney 2003) or even lower at 50 μatm under the sea-ice (Gibson and Trull 1999) up to values of 410 μatm which have been observed during the austral winter during a multiyear time series, clearly showing oversaturation in comparison to the average atmospheric pCO_2 of 357 μatm (Takahashi et al. 2009). Upwelling deep waters may comprise even more CO_2 and values of pCO_2 as high as 450 μatm have been observed in surface waters around the tip of the Antarctic Peninsula (Steven van Heuven, personal communication).

Due to the uptake of anthropogenic CO_2 by the oceans this natural range is likely to show a general increase in the near future. The A1B scenario (moderate growth, balanced across energy sources scenario) of the Intergovernmental Panel on Climate Change (IPCC) predicts an atmospheric CO_2 concentration of approximately 500–600 μatm for the years 2045–2070, and for the worst case scenario (A1F1) already in the years 2040–2055 (Meehl et al. 2007). Surface waters in close equilibrium with the atmosphere, may have similar apparent pCO_2 values. This implies that Southern Ocean phytoplankton today and in the future until 2070 may experience a tenfold range (50–450 or 600 μatm, respectively) in pCO_2. Since the true $CO_{2(aq)}$ is proportional (given that salinity and temperature remain constant) to the apparent pCO_2, this will also have a tenfold range from approximately 3 to 33 $\mu mol \cdot kg^{-1}$.

Aqueous CO_2 is the only chemical form of inorganic carbon that can be fixed by the carboxylating enzyme ribulose-1,5-biphosphate carboxylase/oxygenase (RuBisCO). Therefore, the large variability in the $CO_{2(aq)}$ can have conceivable effects on the physiology and CO_2 fixation by phytoplankton. Large diatom species are important actors in the cycling of carbon and other major nutrients by uptake, settling, and remineralisation. *Proboscia alata* (Brightwell) Sundström is a large cylindrical pennate Southern Ocean diatom. It has been found in several areas of the Southern Ocean, such as in the Atlantic sector and near Kerguelen Island and Heard Island in the Indian Ocean sector, where it is a common and in some regions a dominant species, representing up to 10% of the total biomass (Assmy et al. 2007, Armand et al. 2008). In the sea ice of Wood Bay it has been found in abundances up to 320 cells $\cdot L^{-1}$ (Moro et al. 2000). Furthermore, it has been studied extensively for its membrane lipids, which are strongly affected by temperature and upwelling conditions, and can therefore be used as a proxy for paleoclimate reconstruction (Rampen et al. 2007, 2009). The widespread presence of this diatom in the Southern Ocean and its use for paleoclimate reconstruction makes *P. alata* an important species to study.

As a first assessment of the response of phytoplankton to combined effects of light climate and CO_2 conditions, we have chosen to study *P. alata* under two light conditions, at 40 $\mu mol \cdot photons \cdot m^{-2} \cdot s^{-1}$ (low light, LL) and 240 $\mu mol \cdot photons \cdot m^{-2} \cdot s^{-1}$ (high light, HL). For both light conditions three $CO_{2(aq)}$ concentrations were tested, ranging from low $CO_{2(aq)}$ (8–9 $\mu mol \cdot kg^{-1}$, 137–155 μatm), intermediate $CO_{2(aq)}$ (11–14 $\mu mol \cdot kg^{-1}$, 202–253 μatm), and high $CO_{2(aq)}$ (28–33 $\mu mol \cdot kg^{-1}$, 511–598 μatm).

MATERIALS AND METHODS

Medium and culture conditions. Prior to the experiment, *Proboscia alata* (Brightwell) Sundström (laboratory strain, NIOZ culture collection, unknown origin) was cultured in aged, natural seawater originating from the Bay of Biscay (Timmermans et al. 2001). This seawater was filter sterilized over a Sartobran 105 filter (pre-filter 0.45 μm and end-filter 0.20 μm pore size). Nutrient stocks were made of Na_2SiO_4, $NaNO_3$, NaH_2PO_4, and $FeCl_3*6H_2O$ (Merck, Germany), respectively, diluted in Milli-Q and sterilized by microwaving before adding to the filtered seawater (final concentrations 60 μM Si, 60 μM NO_3^-, 3.75 μM PO_4^{3-}), mimicking nutrient replete conditions. Iron was added to a final concentration of 5 μM, resulting in Fe replete growth conditions. Other essential trace elements were added to final concentrations of: Zn 0.01 μM, Co 0.01 μM, Cu 0.04 μM, and Mn 0.45 μM. Ethylenediaminetetraacetic acid (EDTA) was added (5.86 μM) to keep the nutrients in solution. The stock cultures were regularly diluted with this medium over a period of 15 months prior to the experiment to maintain high growth rates, and at least 1 week before inoculation, the diatoms were transferred to fresh culture medium again, to start the experiments with healthy growing diatoms. The stock cultures of the diatoms were kept at 3°C (±1°C), under a light:dark regime of 16:8 h and daily stirring by hand kept the cells in suspension.

Experimental cultures. During the experiment, which lasted for 37 d, the diatoms were cultured in 6 L polymethylmetacrylate (PMMA) culture vessels, one for each treatment, which were co-designed with and constructed by the NIOZ workshop (a manuscript with a detailed description of the vessels is in preparation). To ensure a constant temperature of 3.0°C in the culture vessels, these were water jacketed and connected to thermostat baths (Lauda Ecoline StarEdition RE 104). Irradiance (measured with a QSL PAR irradiance sensor [Biospherical Instruments Inc., San Diego, CA, USA]) in the culture vessels filled with seawater was 240 $\mu mol \cdot photons \cdot m^{-2} \cdot s^{-1}$ (HL: high light cultures) or 40 $\mu mol \cdot photons \cdot m^{-2} \cdot s^{-1}$ (LL: low light cultures), in a 16:8 h L:D cycle, provided by Biolux cool daylight lamps (Philips TL-D 965/18W). Continuous aeration of the cultures with 3 different mixtures of pCO_2 in natural air (HiQ-Line Linde gas Benelux, Schiedam, the Netherlands), resulted in three different treatments (low, intermediate and high $CO_{2(aq)}$), for each light condition (see Table 1).

Continuous stirring (approximately 50 rpm) of the culture medium kept the cells in suspension and prevented the diatoms from adhering on the walls of the culture vessel. Initial cell abundances of the pre-culturing phase (Fig. 1) were approximately 10 cells $\cdot mL^{-1}$.

The cultures were grown in batches through one complete growth phase, to determine the lag phase, the exponential phase, and the start of the senescent phase. Furthermore, this

TABLE 1. The parameters of the carbonate system in the cultures at 3.0°C.

	$A_{T(measured)}$ ($\mu mol \cdot kg^{-1}$)	$A_{T(expected)}$ ($\mu mol \cdot kg^{-1}$)	DIC ($\mu mol \cdot kg^{-1}$)	pCO_2 (μatm)	$CO_{2(aq)}$ ($\mu mol \cdot kg^{-1}$)	HCO_3^- ($\mu mol \cdot kg^{-1}$)	CO_3^{2-} ($\mu mol \cdot kg^{-1}$)	pH
Low CO_2 HL	2518 (±4)	2513 (±2)	2141 (±6)	135 (±5)	8 (±0)	1875 (±11)	258 (±6)	8.47 (±0.01)
Intermediate CO_2 HL	2520 (±4)	2516 (±3)	2229 (±12)	200 (±9)	11 (±1)	2016 (±18)	202 (±6)	8.33 (±0.02)
High CO_2 HL	2528 (±3)	2526 (±6)	2428 (±7)	599 (±40)	33 (±2)	2307 (±10)	88 (±5)	7.91 (±0.03)
Low CO_2 LL	2517 (±4)	2515 (±7)	2167 (±6)	152 (±6)	8 (±0)	1919 (±12)	240 (±6)	8.43 (±0.02)
Intermediate CO_2 LL	2515 (±3)	2508 (±2)	2266 (±3)	246 (±6)	14 (±0)	2078 (±5)	175 (±3)	8.25 (±0.01)
High CO_2 LL	2532	2529	2407	506	28	2277	102	7.98

Total alkalinity ($A_{Tmeasured}$), and dissolved inorganic carbon (DIC) were measured. The expected total alkalinity ($A_{T(expected)}$) was also calculated from the A_T in the supply vessels corrected for nitrate uptake. Using $A_{T(measured)}$ and DIC, the other variables pCO_2, $CO_{2(aq)}$, CO_3^{2-}, and HCO_3^-, were calculated. Data are presented as the average value (±standard deviation). $n = 6$, except for high CO_2 LL, where $n = 1$.

HL, high light conditions; LL, low light conditions.

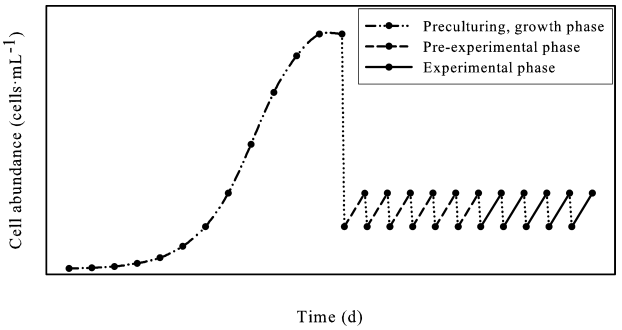

FIG. 1. Typical cell abundance during the different phases of the $CO_{2(aq)}$ and light manipulation experiments with *P. alata*. The dash-dot-dot line shows the complete growth curve that was followed at the start of the experiment, the dotted line shows the dilution phase, where three times the culture volume was exchanged and the thick continuous line shows the experimental phase. Dotted lines show the dilutions between the growth periods. The actual cell abundance data can be found in the supporting material (Fig. S1).

period of 21 d (5 generations) allowed the cells to adapt to the new conditions. After that the cultures were grown semi-continuously during the pre-experimental phase of 11 d (8–10 generations) (see Fig. 1 for a schematic overview of the experiment and Fig. S1 in the supporting material for the data). Daily dilutions with pre-equilibrated (with the desired $CO_{2(aq)}$) supply medium ensured that the cells kept growing exponentially and culturing conditions remained constant to prevent physiological artefacts due to, for example nutrient limitation. During the 11 d of the pre-experimental phase, the volume of the culture was exchanged three times in total with supply medium. Cell abundance in the cultures was determined by microscopy as described below and fresh medium was added to keep the cell abundance constant between approximately 50 and 90 cells $\cdot$ mL^{-1}. This resulted in daily dilutions ranging from the addition of no fresh medium to approximately 40% of the culture volume being replaced with fresh medium at the start of the dilution series, stabilizing to approximately 25% replacement at the end of the pre-experimental phase. During the next 5 d (4 generations), the experimental phase (Figs. 1 and S1), the cultures were again diluted on a daily basis, keeping the cell abundance constant at 35–70 cells $\cdot$ mL^{-1}. The average daily replacement of culture volume was 25% (±13%), this did not include the high CO_2 LL culture, which ceased growing after two dilutions in the pre-experimental phase and could not be diluted any further. Several parameters were sampled before and after dilution: cell abundance, morphology (cell size and cell shape), F_0 (autofluorescence) and F_M (maximum fluorescence), photosynthetic efficiency (F_V/F_M), and dissolved inorganic nutrient concentrations (nitrate, phosphate and silicate). In addition, before dilution the chlorophyll *a* concentration, organic carbon concentrations, and inorganic carbon were sampled as well. Daily sampling was done at the same time (±30 min) during the diurnal light cycle of the cultures. The high CO_2 LL culture was only sampled for nutrients, cell abundance, and photosynthetic efficiency on a daily basis, all other parameters were only sampled once, at the end of the experiment, using the remaining culture volume in the culture vessel.

Inorganic carbon. For the determination of the inorganic carbon system, 250 mL samples were taken from both culture and supply vessels and fixed with 50 μL $HgCl_2$, closed and stored according to Dickson and Goyet (1994) and Dickson et al. (2007). Total alkalinity and total inorganic carbon were determined with a VINDTA 3C (Versatile INstrument for the Determination of Total inorganic carbon and titration Alkalinity, Marianda, Germany). Every analytical series included the determination of certified reference material (CRM) (Dickson et al. 2007). The precision of the DIC and A_T measurements was 7.2 $\mu mol \cdot kg^{-1}$ and 1.7 $\mu mol \cdot kg^{-1}$, respectively, versus the reference standard. The speciation of $CO_{2(aq)}$, HCO_3^-, and CO_3^{2-}, and the derived variables pCO_2 and pH were calculated from A_T and DIC, following Lewis and Wallace (1998) using CO_2 dissociation constants of Mehrbach et al. (1973) refitted by Dickson and Millero (1987), the CO_2 solubility coefficient of Weiss (1974), the borate acidity constant of Dickson (1990b), and the SO_4^{2-} dissociation constant of Dickson (1990a). Salinity, silicate, and phosphate concentrations were incorporated in the calculations. To test for possible DOC effects on A_T (Kim and Lee 2009), the measured A_T ($A_{T(measured)}$) was compared with the expected A_T ($A_{T(expected)}$). The $A_{T(expected)}$ was calculated from the measured A_T of the supply vessels with correction for nitrate uptake in the cultures (Brewer and Goldman 1976).

Morphology and specific growth rates. The morphology and cell abundance of the cultures were determined with a Zeiss Axiovert 200 inverted microscope (with an Axiocam MRc camera, Carl Zeiss MicroImaging GmbH, Jena, Germany). For morphology, a total of 10 samples were counted for each culture, except the high CO_2 low light culture, which was counted seven times. A distinction was made between regular cells and cells which formed spirals. Regular cells were determined to be rectangular, with the characteristic proboscis of *P. alata* on both ends. Cells that completed at least one full circle were distinguished as spirals. Fragmented cells in the high CO_2 cultures were not quantified, since it was not possible to determine in how many parts the cells disintegrated. Cell

size (length and diameter) was only determined for the regular shaped cells. Approximate cell volume ($V_{Proboscia}$) was calculated from the length (l) and radius (r) of the cells, following the equation: $V = \pi \cdot r^2 \cdot l$. When the diatoms formed chains, single cells were counted separately as these could be easily distinguished. Cell abundance, both before and after dilution, was determined daily at the same time (±30 min) during the light cycle in a 6 mL settling chamber. The dilution factor was determined by the cell abundance before dilution. A minimum of 200 cells per sample was counted and counts were done in triplicate. Specific growth rates per day were calculated from the different incubations, by linear regression of the natural logarithm of the cell abundance during exponential growth.

Silicate speciation. The chemical equilibrium model used for silicate speciation calculations was Mineql + 4.6.1 (Secher and McAvoy 2007). The composition of the seawater was calculated from the composition of the culture medium. The stability constants of the software were used and the average measured DIC and calculated pH (from DIC and A_T) were incorporated in the calculations, as was the average silicate concentration in each of the cultures. Precipitation was allowed in the model.

Photosynthetic efficiency and Chlorophyll a. Triplicate samples for the determination of the photochemical quantum efficiency (F_V/F_M) were taken during the light period of the cultures and stored in the dark at 4°C for at least 5 min prior to the actual measurements (to allow dark-adaptation of samples). After that, the F_0 (chlorophyll *a* autofluorescence), F_M (maximum chlorophyll *a* fluorescence), and F_V/F_M (photochemical quantum efficiency, where $F_V = F_M - F_0$) were determined with a PAM fluorometer (Pulse Amplitude Modulated-CONTROL Universal Control Unit, WATER-mode, Walz, Germany).

For the determination of Chlorophyll *a,* 150 mL samples were filtered over a 0.7 μm pore size GF/F filter (glass fibre filter, diameter 25 mm), under low light conditions. Filters were stored at −80°C. Prior to analysis, the filters were extracted overnight in 10 mL of 90% acetone at −20°C. Analysis of chlorophyll *a* was done with a SpectraMax M2 spectrofluorometer (with SoftMax Pro software, Molecular Devices, Sunnyvale, CA, USA). Fluorescence of the samples was measured and chlorophyll *a* concentrations were determined against a standard chlorophyll *a* solution according to the protocol designed by Holm-Hansen et al. (1965).

Organic carbon and nitrogen. Organic carbon was sampled in three fractions; total organic carbon (TOC), particulate organic carbon (POC), and dissolved organic carbon (DOC). Organic nitrogen was only sampled as particulate organic nitrogen (PON). For POC and PON analysis 150 mL samples were filtered over a pre-combusted 0.7 μm pore size GF/F filter (diameter 12 mm). Filters were stored at −80°C. Prior to POC analysis, the filters were freeze dried. Analysis of POC and PON was done with a Thermo-Interscience Flash EA1112 Series Elemental analyzer, according to an adapted protocol of Verardo et al. (1990) and corrected for blanks. The POC and PON values were normalized to cell abundance and expressed in $\mu mol \cdot cell^{-1}$. Twenty milliliter of filtrate of the POC and PON sampling was sampled for DOC. The DOC (filtrate) and TOC (20 mL unfiltered sample) were sampled in duplicate, acidified with 3 drops of 85% H_3PO_4, and stored in pre-combusted glass ampoules.

Analysis of TOC and DOC was done with a Total Organic Carbon Analyzer, Model TOC-V CPH/CPN (Shimadzu Corporation, Kyoto, Japan) (six injections). Concentrations of TOC and DOC were determined against deep seawater reference material, batch 8 lot no. 12, from the Hansell Laboratory (University of Miami, RSMAS). The high CO_2 LL culture was sampled only once for POC, PON, TOC, and DOC.

Nutrients. Nutrient samples were filtered over a 0.2 μm filter (Acrodisc®, 32 mm syringe filter, Supor® membrane, membrane, Pall Cooperation, Newquay, Cornwall, UK) in 6 mL polyethylene Pony Vials™ (PerkinElmer Life and Analytical Sciences, Shelton, CT, USA). The filter and syringe were rinsed three times with MilliQ and once with sample. The Pony Vials were rinsed three times with filtered sample. Although the filters were not clogged after filtering 12 samples because of the low cell abundance in the cultures, they were replaced on a daily basis to prevent drying of the filter or growth of microorganisms on the filter. The filtered samples were stored at 4°C (dissolved silicate) and −20°C (nitrate and phosphate) until further analysis. Dissolved nutrient concentrations were determined on a TRAACS Auto Analyzer 800+ (Bran+Luebbe, Norderstedt, Germany) with the use of spectrophotometric methods (Grasshoff et al. 1983). Nutrient uptake was calculated from nutrient concentrations in the cultures before and after dilution and normalized to cell counts, expressed as $pmol \cdot cell^{-1} \cdot d^{-1}$.

Statistical analysis. All statistical analyses were done using SPSS 13.0 (SPSS Inc., Chicago, IL, USA). A parametric test was used when the assumptions for parametric tests (homogeneity of variances and a normal distributed data set) were met. In other cases, non-parametric tests were used. Due to the combination of two experimental parameters (light and $CO_{2(aq)}$) we used the analysis of covariance (ANCOVA) to discern out which effects were most likely being caused by light and/or $CO_{2(aq)}$ (Field 2007). Because of the ceased growth in the high CO_2 LL culture, results of this culture were left out of the statistical analyses, but are presented as averages (± standard deviation) where possible.

RESULTS

Inorganic carbon. The inorganic carbon data showed that the experiments were consistent with respect to the carbonate system (Table 1). The variation in A_T within the cultures over the experimental period of 6 d was small, with a maximum standard deviation of 5 $\mu mol \cdot kg^{-1}$ for each treatment. A linear regression between the measured A_T ($A_{Tmeasured}$) and the expected A_T ($A_{Texpected}$) showed that there was a good correlation between the two ($\tau = 0.515$, $P \ll 0.001$). The $A_{T(expected)}$ was on average 0.93 $\mu mol \cdot kg^{-1}$ lower than $A_{T(measured)}$, a small difference that is well below the analytical error, hence not significant (Fig. S2 in supporting material). Comparing $\Delta A_{T(measured\text{-}expected)}$ to the DOC concentrations revealed a slight negative correlation ($y = -0.24x + 30.59$, $\tau = -0.522$, $P \ll 0.001$) (Fig. S3 in supporting material).

The DIC data of the cultures showed that this parameter was also consistent within each culture vessel, with a maximum standard deviation of 14 $\mu mol \cdot kg^{-1}$ (Table 1). The calculated pCO_2 values of these samples showed that continuous aeration of the cultures resulted in an average pCO_2 between 137 and 598 μatm, corresponding to an average pH between 7.9 and 8.5 (Table 1).

Morphology and specific growth rate. A clear effect of the different $CO_{2(aq)}$ treatments was a change in morphology of the *P. alata* cells (Fig. 2). In the low CO_2 HL cultures, chains of *P. alata* started to form spirals (Fig. 2, A–C). A significant 7.5% (±4.2%) of the cells in this culture, showed this spiral shape, compared to 0.3 (±0.5%) in the intermediate CO_2

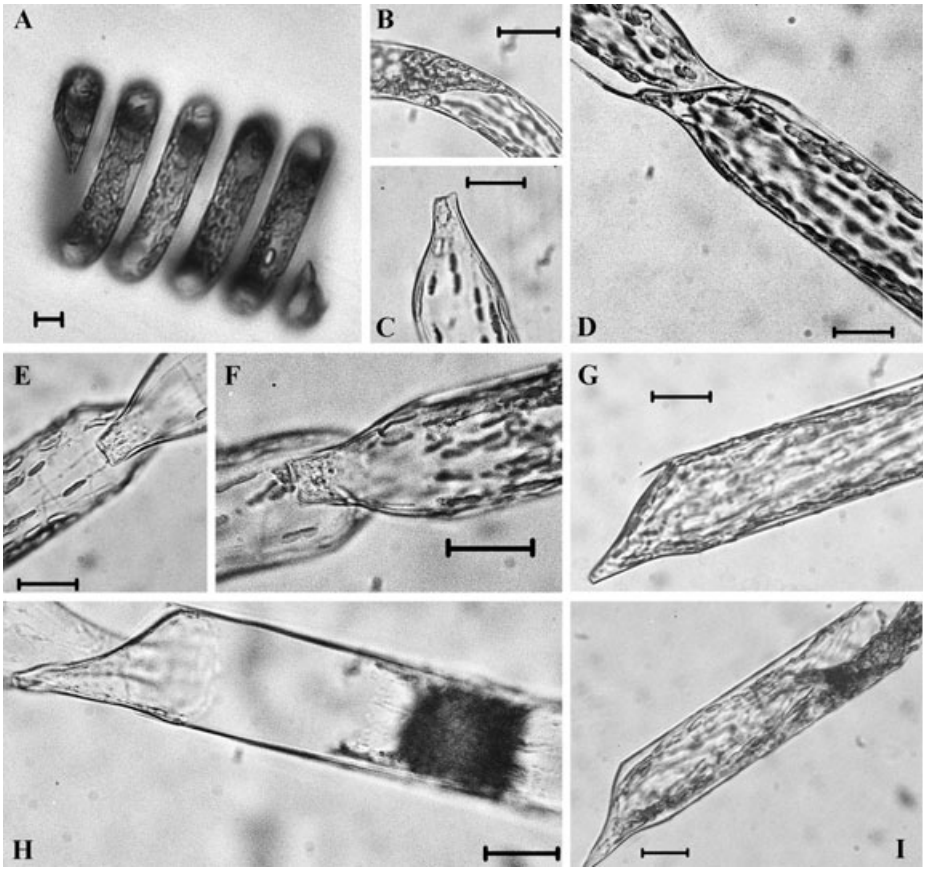

FIG. 2. (A–I) Different morphology of *P. alata* in the different light and $CO_{2(aq)}$ treatments, (A–C) low $CO_{2(aq)}$ HL, (D) low $CO_{2(aq)}$ LL (E–F) intermediate $CO_{2(aq)}$ HL, (G) intermediate $CO_{2(aq)}$ LL, (H) high $CO_{2(aq)}$ HL and (I) high $CO_{2(aq)}$ LL. Scale bar 10 μm.

HL and 0.4% (±0.7%) in the low CO_2 LL culture. For none of these cultures a trend over time was observed (low CO_2 HL: $r^2 = 0.00$, intermediate CO_2 HL: $r^2 = 0.18$, low CO_2 LL: $r^2 = 0.13$). In the high CO_2 cultures, both the HL and LL culture, cell structure deteriorated, leading to cell fragmentation (Fig. 2, H–I). There was no chain formation in these cultures. Chain formation only took place in the cultures that were grown in intermediate and low $CO_{2(aq)}$ conditions under both HL and LL.

Cell length of the regular shaped cells varied, ranging from 104.6 μm in length (intermediate CO_2 LL) to 877.9 μm (low CO_2 LL). The latter was one very large cell which only occurred once. Cell length and diameter did not vary significantly between the 6 different treatments, however, within different treatments there were significant differences. In HL conditions, cell diameter decreased with increasing $CO_{2(aq)}$ ($\tau = -0.105$ $P = 0.007$). This led to a significant decrease in cell volume with increasing $[CO_{2(aq)}]$ ($\tau = -0.081$ $P = 0.035$). Cells treated in the high CO_2 conditions at low light were the largest, 271 μm (±56 μm) (Table 2).

Average specific growth rates in the HL cultures per culture were: 0.55, 0.58, and 0.52 d^{-1} for low, intermediate, and high CO_2, respectively. Growth rates in the LL cultures were 0.67, 0.57, and 0.19 d^{-1} for low, intermediate, and high CO_2 conditions (Fig. 3). Growth rates were not statistically significant influenced by the different light ($F_{(1,18)} = 0.559$, $P = 0.464$) and $CO_{2(aq)}$ (HL: $\tau =$

TABLE 2. Average (±standard deviation) cell size of *P. alata* in the different treatments.

	Length (μm)	Diameter (μm)	Volume (10^3 μm^3)
Low CO_2 HL ($n = 97$)	219.9 (±54.2)	28.5 (±2.0)	142.4 (±46.1)
Intermediate CO_2 HL ($n = 111$)	257.4 (±68.7)	27.9 (±2.3)	159.7 (±54.3)
High CO_2 HL ($n = 121$)	223.7 (±54.4)	27.8 (±2.0)	137.2 (±42.9)
Low CO_2 LL ($n = 130$)	263.5 (±97.5)	28.5 (±2.4)	170.7 (±73.4)
Intermediate CO_2 LL ($n = 110$)	229.5 (±78.2)	29.1 (±2.7)	154.1 (±59.5)
High CO_2 LL ($n = 43$)	271.2 (±56.3)	29.5 (±2.2)	188.0 (±54.4)

Aqueous CO_2 concentrations as indicated in materials and methods and results.

HL, high light; LL, low light.

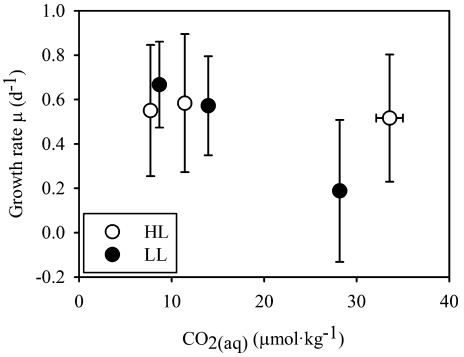

FIG. 3. Growth rates (μ, d^{-1}, $n = 4$) of *P. alata* during the experiment versus the average $CO_{2(aq)}$ concentration between dilutions. Open circles denote the HL cultures, closed circles denote LL cultures. Error bars denote the standard deviation.

TABLE 3. The average photochemical quantum efficiency (F_V/F_M) (±standard deviation, $n = 8$ except for high CO_2 LL, $n = 5$) and the average chlorophyll *a* concentration (±standard deviation ng · $cell^{-1}$, $n = 5$, except for 750 μatm LL, $n = 1$) of the *P. alata* cells in the different treatments.

	F_V/F_M	Chlorophyll *a* (pg · $cell^{-1}$)
Low CO_2 HL	0.67 (±0.02)	97.1 (±6.6)
Intermediate CO_2 HL	0.69 (±0.03)	99.1 (±14.6)
High CO_2 HL	0.68 (±0.03)	104.9 (±12.4)
Low CO_2 LL	0.69 (±0.05)	109.8 (±12.9)
Intermediate CO_2 LL	0.69 (±0.05)	91.4 (±16.5)
High CO_2 LL	0.67 (±0.04)	540.3

The $CO_{2(aq)}$ concentrations as indicated in materials and methods and results.

HL, high light; LL, low light.

0.091 $P = 0.681$ and LL: $\tau = 0.086$ $P = 0.752$) treatments. After diluting the high CO_2 LL culture twice in the pre-experimental phase, cell abundance decreased to 90 cells · mL^{-1} and kept decreasing further to 40 cells · mL^{-1} without being diluted. At the start of the experiment cell abundance in the high CO_2 LL culture was stable at approximately 29 (±8) cells · mL^{-1} and the very low growth rates prevented dilution of the culture.

Silicate speciation. The calculations showed that silicate speciation was influenced by the different $CO_{2(aq)}$ concentrations. The non-dissociated $Si(OH)_4$ species increased from 97% to 99% of the total average silicate concentration in each culture vessel, with increasing $[CO_{2(aq)}]$. On the other hand, the partially dissociated $H_3SiO_4^-$ and $H_2SiO_4^{2-}$ decreased with increasing $[CO_{2(aq)}]$. In the high $CO_{2(aq)}$ cultures there was 3 times less $H_3SiO_4^-$ available compared with the low $CO_{2(aq)}$ culture (approximately 1.3 μM in low $CO_{2(aq)}$ and approximately 0.4 μM high $CO_{2(aq)}$ cultures). Furthermore, there was approximately 10 times less $H_2SiO_4^{2-}$ available in the high $CO_{2(aq)}$ culture than in the low $CO_{2(aq)}$ cultures (respectively, approximately 1.4 pM and approximately 17.9 pM) (Fig. S4 in supporting material).

Photosynthetic efficiency and Chlorophyll a. The photochemical quantum efficiency (F_V/F_M), was high in all cultures, ranging from 0.67 (±0.04) in high CO_2 LL to 0.69 (±0.05) in low CO_2 LL (Table 3). A slightly higher F_V/F_M was observed in the cultures growing in LL conditions (not significant $U = 144.00$, $r = -0.248$) except for the cells cultured in high $CO_{2(aq)}$. These cells showed a slightly lower F_V/F_M. Non-parametric correlation analysis showed that there was no significant correlation between the $[CO_{2(aq)}]$ and the F_V/F_M ($\tau = -0.018$, $P = 0.901$ and $\tau = -0.206$, $P = 0.249$, HL and LL, respectively).

The chlorophyll *a* concentration per cell did not differ between the different light treatments ($U = 44.00$, *ns*, $r = -0.069$). Chlorophyll *a* concentrations in the HL cultures ranged between 97 and 104 pg · $cell^{-1}$, while concentrations is LL conditions ranged between 91 and 110 pg · $cell^{-1}$. There was also no significant difference of chlorophyll *a* between the three different $CO_{2(aq)}$ treatments ($\tau = 0.182$, $P = 0.411$ and $\tau = -0.500$, $P = 0.083$) (Table 3). As mentioned above, the cells that were cultured in low light and high $CO_{2(aq)}$ were excluded from this statistical comparison, yet this culture contained five to six times more chlorophyll *a* per cell in comparison with the cells in the five other treatments (540 pg · $cell^{-1}$).

Organic carbon and nitrogen. A significant effect of the light treatments on TOC concentrations (μmol · L^{-1}) was found. The high light cultures showed higher TOC concentrations than the low light cultures ($F_{(1,22)} = 18.142$, $P \ll 0.001$). A similar effect of $[CO_{2(aq)}]$ on TOC (μmol · L^{-1}) was found in both the HL ($\tau = 0.543$, $P = 0.005$) and the LL cultures ($\tau = 0.289$, $P = 0.245$) (Fig. 4A). The DOC concentrations (μmol · L^{-1}) were neither affected by the two different light treatments ($F_{(1,20)} = 0.404$, $P = 0.532$), nor by the $[CO_{2(aq)}]$ (HL: $\tau = 0.275$, $P = 0.17$, LL: $\tau = 0.167$, $P = 0.532$) (Fig. 4B). On the other hand, both the cellular POC (μmol · $cell^{-1}$) and PON (μmol · $cell^{-1}$) were significantly higher in the HL cultures than in the LL cultures (POC: $F_{(1.14)} = 26.691$ $P \ll 0.001$ and PON: $F_{(1.14)} = 46.778$, $P \ll 0.001$) (Fig. 4, C and D). The cellular POC contents (μmol · $cell^{-1}$) showed a significant positive correlation with $[CO_{2(aq)}]$ ($\tau = 0.778$, $P = 0.004$) in the HL cultures and a significant decrease in organic carbon per cell in the LL cultures ($\tau = -0.714$, $P = 0.013$). A similar response was found for cellular PON content (HL: $\tau = 0.722$, $P = 0.007$; LL: $\tau = -0.643$, $P = 0.026$) (Fig. 4D). The POC:PON ratio was also found to be significantly influenced by the light treatment, with the POC:-PON ratio being higher in LL cultures ($F_{(1.14)} = 22.879$, $P \ll 0.001$). In the HL cultures, POC:PON ratios ranged between 7.9 (±0.2) and 9.2 (±0.2) for the low and high CO_2 cultures, respectively, which was a significant increase with increasing $[CO_{2(aq)}]$ ($\tau = 0.412$, $P = 0.021$). In the LL

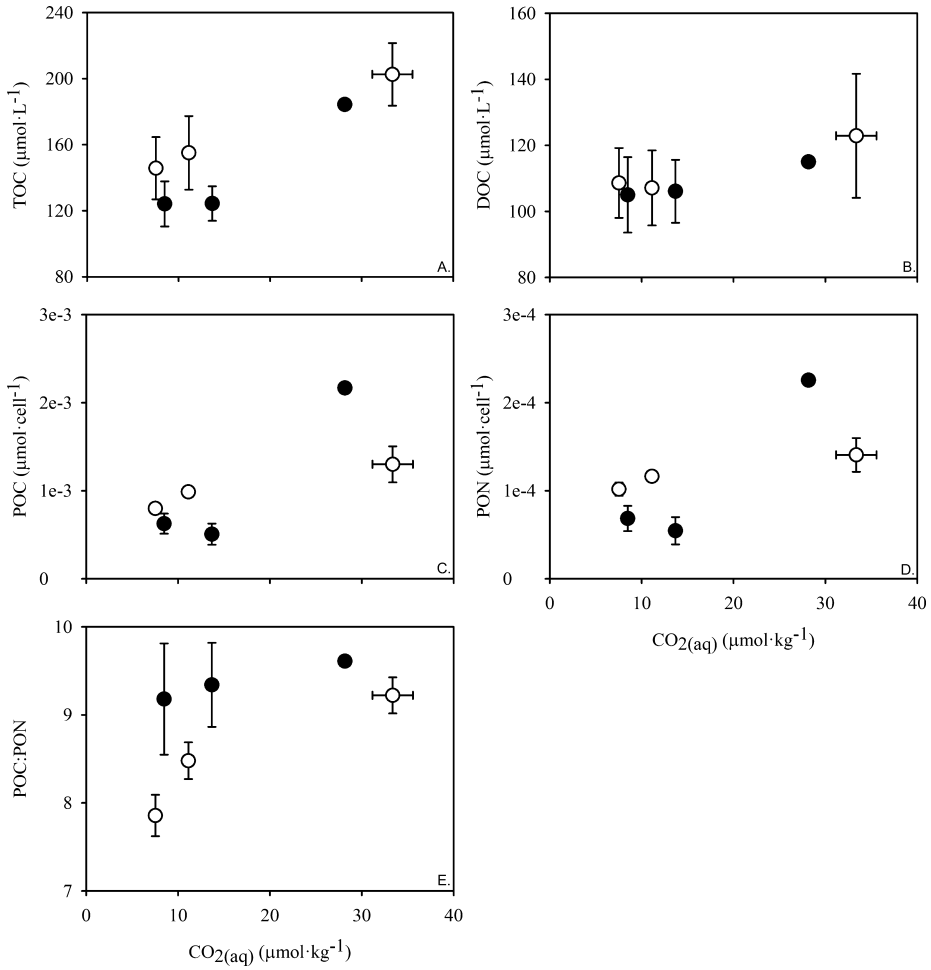

FIG. 4. (A–E) Total, dissolved and particulate organic carbon and particulate organic nitrogen versus the $CO_{2(aq)}$ concentration. Open symbols denote the HL cultures, closed symbols the LL cultures. Error bars denote the standard deviation ($n = 3$ for the HL cultures, $N = 4$ for low and intermediate CO_2 LL cultures and $n = 1$ for the high CO_2 LL culture). A.) TOC ($\mu mol \cdot L^{-1}$) concentrations in the different treatments. B.) DOC ($\mu mol \cdot L^{-1}$) concentrations in the different treatments. C.) POC ($\mu mol \cdot cell^{-1}$) contents in the different treatments. D.) PON ($\mu mol \cdot cell^{-1}$) contents in the different treatments. E.) POC:PON ratio in the different treatments.

cultures, POC:PON ratios ranged between 9.2 (±0.8) and 9.6 for the low and high CO_2 cultures, respectively, and were not influenced by $[CO_{2(aq)}]$ (Fig. 4E).

The POC ($\mu mol \cdot cell^{-1}$) and PON ($\mu mol \cdot cell^{-1}$) concentrations in the high CO_2 LL culture were much higher than that of the high CO_2 HL culture ($2.17 \cdot 10^{-3}$ compared to $1.30 \cdot 10^{-3} \pm 2.04 \cdot 10^{-5}$ $\mu mol \cdot cell^{-1}$, respectively). The PON ($\mu mol \cdot cell^{-1}$) in the high CO_2 LL cultures was also much higher than in the high CO_2 HL; $2.26 \cdot 10^{-4}$ compared to $1.41 \cdot 10^{-4}$ ($\pm 1.91 \cdot 10^{-5}$) $\mu mol \cdot cell^{-1}$ (Fig. 4D). The TOC and DOC concentrations in the high CO_2 LL culture were similar to the high CO_2 HL culture.

Nutrient uptake. Nutrient concentrations were kept constant during the experiment. For phosphate, the minimum concentration measured was 1.72 $\mu mol \cdot L^{-1}$ and the maximum concentration was 2.54 $\mu mol \cdot L^{-1}$. The lowest nitrate concentration measured was 40.48 $\mu mol \cdot L^{-1}$; and the highest concentration was 47.27 $\mu mol \cdot L^{-1}$. Silicate concentrations ranged between 39.97 and 47.03 $\mu mol \cdot L^{-1}$. These values do not include the nutrient measurements in the high CO_2 LL culture. Here, nutrient concentrations decreased, while there was no increase in cell numbers observed. In this high CO_2 LL culture, phosphate decreased from 1.70 to 1.29 $\mu mol \cdot L^{-1}$, nitrate from 37.29 to 31.06 $\mu mol \cdot L^{-1}$ and silicate decreased from 38.93 to 32.60 $\mu mol \cdot L^{-1}$.

The effects of light and $CO_{2(aq)}$ on nutrient uptake and molar nutrient uptake ratios were calculated without including the high CO_2 LL culture. The average nitrate uptake in the treatments ranged between 49 and 144 $pmol \cdot cell^{-1} \cdot d^{-1}$ (Table 4), while average phosphate uptake ranged between 3 $pmol \cdot cell^{-1}$ and 17 $pmol \cdot cell^{-1} \cdot d^{-1}$, and average silicate uptake ranged between 106 and 225 $pmol \cdot cell^{-1} \cdot d^{-1}$. For all three nutrients the highest uptake rates were found in the HL cultures. Both in the HL and LL cultures the nutrient uptake

TABLE 4. Average (±standard deviation) nutrient uptake ($pmol \cdot cell^{-1} \cdot d^{-1}$) and nutrient uptake ratios in the different light and $CO_{2(aq)}$ treatments.

	ΔNitrate	ΔPhosphate	ΔSilicate	N:P ratio	N:Si ratio	Si:P ratio
Low CO_2 HL	108 (±67)	12 (±5)	157 (±69)	8.33 (±1.54)	0.66 (±0.12)	12.73 (±1.22)
Intermediate CO_2 HL	124 (±64)	14 (±8)	195 (±95)	9.46 (±2.28)	0.62 (±0.05)	15.01 (±3.60)
High CO_2 HL	144 (±51)	17 (±6)	225 (±83)	8.66 (±1.19)	0.64 (±0.03)	13.47 (±1.32)
Low CO_2 LL	57 (±23)	3 (±2)	140 (±111)	20.04 (±5.4)	0.53 (±0.21)	47.37 (±31.62)
Intermediate CO_2 LL	49 (±22)	3 (±3)	106 (±42)	10.98 (±5.06)	0.45 (±0.08)	23.97 (±11.35)
High CO_2 LL	428 (±367)	31 (±31)	392 (±289)	13.43 (±2.41)	1.02 (±0.18)	13.49 (±4.09)

The $CO_{2(aq)}$ concentrations are indicated in materials and methods and results. For nutrient uptake: $n = 5$ except intermediate CO_2 LL culture ($n = 4$) and high CO_2 LL ($n = 3$) For nutrient uptake ratios: N:P $n = 5$ except low CO_2 LL ($n = 4$) and intermediate and high CO_2 LL ($n = 2$). N:Si $n = 5$ except high CO_2 LL ($n = 4$). Si:P $n = 5$ except intermediate CO_2 LL ($n = 2$) and high CO_2 LL ($n = 3$).

HL, high light; LL, low light.

rates were not significantly influenced by $[CO_{2(aq)}]$ (HL: $\tau = 0.091$, $P = 0.681$, $\tau = -0.030$, $P = 0.891$ and $\tau = 0.152$, $P = 0.493$ for for Δphosphate, Δnitrate, and Δsilicate, respectively; and LL: $\tau = -0.619$, $P = 0.051$, $\tau = -0.286$, $P = 0.322$ and $\tau = -0.017$, $P = 0.805$ for Δphosphate, Δnitrate, and Δsilicate, respectively).

Molar nutrient uptake ratios for N:P, N:Si, and Si:P were significantly lower in the HL cultures than in LL cultures, (N:P: $F_{(1.13)} = 33.882$, $P \ll 0.001$; Si:P: $F_{(1.13)} = 30.186$, $P \ll 0.001$ and N:Si: $F_{(1.17)} = 6.151$, $P = 0.024$) (Table 4). These ratios were not influenced by the different $CO_{2(aq)}$ concentrations.

DISCUSSION

The major groups of phytoplankton occurring in the Southern Ocean are diatoms, like *P. alata* which was used in the present study, and haptophytes, such as *Phaeocystis antarctica*. Notably the large diatoms are highly significant in the nutrient cycling in major blooms (de Baar et al. 1997, Hoppema and Goeyens 1999, De Baar et al. 2005). Due to the highly variable light conditions in the Southern Ocean, the phytoplankton growth is often limited by light (Mitchell et al. 1991).

Next to the high variability in light, the inorganic carbon concentrations in the modern Southern Ocean are also highly variable, varying from 50 to 450 μatm (Gibson and Trull 1999, Steven van Heuven, personal communication). This large natural variability in inorganic carbon availability and the invasion of anthropogenic CO_2 in oceanic waters has a significant effect on the chemistry of the seawater and could affect the functioning of (photosynthetic) marine organisms. Because the effects of this CO_2 chemistry and its future change on phytoplankton are largely unknown, studying the responses of *P. alata* to different physical and chemical parameters, such as light and $CO_{2(aq)}$ concentrations, might therefore give important clues on its resilience to environmental variability.

During the experiments with *P. alata* the carbonate system in the culture vessels was well maintained. We have found no statistical significant evidence for the previously suggested positive effect of DOC on alkalinity titrations as suggested by Kim and Lee (2009). In fact, if anything, there is a decreasing trend of ΔA_T with increasing [DOC], these differences are, however, small and within the precision and standard deviation of the measurements. The low cell abundance in our experiments may be an explanation for this. If we hypothesize that functional groups of molecules at the outside of phytoplankton cell walls accept some of the protons (H^+) of the acid for A_T titration, we could state that there would be an increasing overestimation of the A_T with increasing cell abundance. This stresses the point that low cell abundances in carbon perturbation experiments are necessary to quantify the carbonate chemistry accurately.

The major finding of this study was the change in morphology of *P. alata* cells. Cell size measurements showed a large variation in cell volume. The measured cell volume of the cultured cells was approximately 10 times larger than the volume of *P. alata* cells found in sea ice (Moro et al. 2000) and particulate organic carbon concentrations of the cells in this experiment were approximately 2–3 times larger than observed in the Southern Ocean (Armand et al. 2008). This is most likely due to the favourable growth conditions in the culture vessels.

Observations on the morphology of the diatoms during the experiment showed remarkable results in response to the culture conditions. The formation of spirals in the low CO_2 HL culture might indicate that the diatoms form a micro-environment in which they optimize the conditions, perhaps increasing the $CO_{2(aq)}$ concentration within the spiral. The formation of spirals was also found in the low CO_2 LL culture, however, this was not significant. To our knowledge this formation of spirals and particular in response to low CO_2 has not been described before.

The response at high $CO_{2(aq)}$ concentrations, the fragmentation of the cells, suggests a deterioration of the silica cell wall. Since the total silica uptake did not significantly change with increasing $[CO_{2(aq)}]$, we hypothesize that this can be ascribed

to a deterioration of the casing, an organic layer around the silica, due to the increased $CO_{2(aq)}$ and therefore decreased pH. The exact composition of this organic casing and how it is formed is not known (van de Poll et al. 1999, Vrieling et al. 2005), but it is likely to prevent the silica cell wall from dissolution in the silica-undersaturated seawater. Deterioration of the casing would lead to dissolution of the cell wall. This has been suggested by Milligan et al. (2004), who also found an increased silica dissolution rate (6- to 7-fold higher) in high CO_2 cultures. This may be an effect also related to the shifts between different chemical forms of the silicate in seawater caused by shifts in the CO_2 controlled pH of seawater. At increasing $CO_{2(aq)}$ this leads to a decrease in the concentration of the partially dissociated $H_3SiO_4^-$ and $H_2SiO_4^{2-}$ ions and an increase in the undissociated $Si(OH)_{4(aq)}$. This decrease in the two dissociated forms of silicate might lead to the fragmentation of the cells, and therefore affect our experimental results. Conversely this would imply that one or both of the dissociated species control dissolution rather than the undissociated $Si(OH)_4$, but it would require novel experiments to validate this hypothesis.

The ceased growth of *P. alata* in the high CO_2 LL culture was remarkable. During the pre-culturing phase the cells grew equally fast as the cells in the other cultures. However, after two dilutions in the pre-experimental phase, growth ceased and cell abundance decreased. The daily photosynthetic yield measurements showed a relatively high F_v/F_m of 0.7, indicating that the cells were efficiently photosynthesizing. Although we could not determine the abundance of fragmented cells, it is possible that the diatoms in the high CO_2 LL culture were dividing, but that cell fragmentation rates almost matched up to the growth rates, therefore resulting in an underestimation of the actual growth rate. This would explain the relatively high F_v/F_m and the continuous nutrient uptake in this culture.

Decreased POC and PON production at increased $[CO_{2(aq)}]$, in the LL cultures (results from high CO_2 LL were not taken into account in this analysis), led to the conclusion that the sequestration of carbon will decrease in LL conditions. In HL conditions this pattern was reversed. The increase in POC concentration per cell, with increasing $[CO_{2(aq)}]$ could be caused by the fragmented cells in the high $CO_{2(aq)}$ culture, which could not be counted. Although these cells are not considered to be viable, there was still organic material present in the fragments. This organic material is included in the analysis of POC, PON (and therefore TOC), and chlorophyll *a*, causing an overestimate of the cell contents. When this high CO_2 HL culture was excluded from the analysis, only the POC concentration and the POC:PON ratio were increasing significantly with increasing $[CO_{2(aq)}]$, concluding that TOC and PON concentrations were not influenced by $[CO_{2(aq)}]$. The increase in POC in *P. alata* cells with increasing $[CO_{2(aq)}]$ at HL conditions suggests an increased carbon sequestration by this species in the future Southern Ocean.

From these results, we conclude that changes in physiology related to future increases of $CO_{2(aq)}$ concentrations are mainly dependent on the light conditions in which these diatoms develop. The predicted future increase in stratification and decreased sea ice cover in the Southern Ocean as a result of global warming will lead to reduced nutrient transport from deeper waters and reduced deep mixing. Phytoplankton will therefore experience longer and higher light conditions (Budd 1991, Bopp et al. 2001). Photoinhibition (Alderkamp et al. 2010, 2011) and nutrient depletion could decrease the primary productivity of *P. alata*.

The authors thank the nutrient laboratory of the Royal Netherlands Institute for Sea Research for analysing the nutrient samples. Santiago Gonzalez is thanked for analysing the total and dissolved organic carbon samples and Sharyn Crayford for analysing the particulate organic nitrogen and carbon samples. Loes Gerringa is thanked for assisting in the silicate speciation calculations. Ika Neven and Peter Boelen and the anonymous reviewers are thanked for reading the manuscript and giving their comments, which helped to improve this manuscript. Funding for this work was provided by the Darwin Center for Biogeology, 5th call, under project number 2061. Additionally, this work is a contribution to the ''European Project on Ocean Acidification'' (EPOCA), which received funding from the European Community's Seventh Framework Programme (FP7/2007–2013) under grant agreement n° 211384.

Alderkamp, A. C., De Baar, H. J. W., Visser, R. J. W. & Arrigo, K. R. 2010. Can photoinhibition control phytoplankton abundance in deeply mixed water columns of the Southern Ocean? *Limnol. Oceanogr.* 55:1248–64.

Alderkamp, A. C., Garcon, V., de Baar, H. J. W. & Arrigo, K. R. 2011. Short-term photoacclimation effects on photoinhibition of phytoplankton in the Drake Passage (Southern Ocean). *Deep Sea Res. Part 1* 58:943–55.

Armand, L. K., Cornet-Barthaux, V., Mosseri, J. & Queguiner, B. 2008. Late summer diatom biomass and community structure on and around the naturally iron-fertilised Kerguelen Plateau in the Southern Ocean. *Deep Sea Res. Part 2 Top. Stud. Oceanogr.* 55:653–76.

Assmy, P., Henjes, J., Klaas, C. & Smetacek, V. 2007. Mechanisms determining species dominance in a phytoplankton bloom induced by the iron fertilization experiment EisenEx in the Southern Ocean. *Deep-Sea Research Part I-Oceanographic Research Papers* 54:340–62.

de Baar, H. J. W., van Leeuwe, M. A., Scharek, R., Goeyens, L., Bakker, K. M. J. & Fritsche, P. 1997. Nutrient anomalies in *Fragilariopsis kerguelensis* blooms, iron deficiency and the nitrate/phosphate ratio (A. C. Redfield) of the Antarctic Ocean. *Deep Sea Res. Part 2 Top. Stud. Oceanogr.* 44:229–60.

Bopp, L., Monfray, P., Aumont, O., Dufresne, J., Le Treut, H., Madec, G., Terray, L. & Orr, J. C. 2001. Potential impact of climate change on marine export production. *Global Biogeochem. Cycles* 15:81–99.

Boyd, P. W., Crossley, A. C., DiTullio, G. R., Griffiths, F. B., Hutchins, D. A., Queguiner, B., Sedwick, P. N. & Trull, T. W. 2001. Control of phytoplankton growth by iron supply and irradiance in the subantarctic Southern Ocean: experimental results from the SAZ Project. *J. Geophys. Res. (Oceans)* 106:31573–83.

Brewer, P. G. & Goldman, J. C. 1976. Alkalinity changes generated by phytoplankton growth. *Limnol. Oceanogr.* 21:108–17.

Budd, W. F. 1991. Antarctica and global change. *Clim. Change* 18:271–99.

De Baar, H. J. W., Boyd, P. W., Coale, K. H., Landry, M. R., Tsuda, A., Assmy, P., Bakker, D. C. E. et al. 2005. Synthesis of iron fertilization experiments: from the iron age in the age of enlightenment. *In* Orr, J. C., Pantoja, S. & Pörtner, H.-O. [Eds.] *The Oceans in High CO2 World*. Special Issue of *J. Geophys. Res. (Oceans)* 110, C09S16, doi:10.1029/2004JC002601, pp 1–24.

Dickson, A. G. 1990a. Standard potential of the reaction - $AgCl_{(S)}+{}^{1}/_{2}H_{2(G)}=Ag_{(S)}+HCl_{(Aq)}$ and the standard acidity constant of the ion HSO_4^- in synthetic sea water from 273.15 K to 318.15 K. *J. Chem. Thermodyn.* 22:113–27.

Dickson, A. G. 1990b. Thermodynamics of the dissociation of boric acid in synthetic seawater from 273.15 K to 318.15 K. *Deep Sea Res. Part A Oceanogr. Res. Pap.* 37:755–66.

Dickson, A. G. & Goyet, C. [Eds.] 1994. *Handbook of Methods for the Analysis of the Various Parameters of the Carbon Dioxide System in sea Water*, Vol. 2. ORNL/CDIAC-74, Prepared for the U.S. Department of Energy, Special Research Grant Program 89-7A, Global survey of carbon dioxide in the oceans, 187 pp.

Dickson, A. G. & Millero, F. J. 1987. A comparison of the equilibrium constants for the dissociation of carbonic acid in seawater media. *Deep-Sea Res. Part A-Oceanogr. Res. Pap.* 34:1733–43.

Dickson, A. G., Sabine, C. L. & Christian, J. R. 2007. *Guide to the Best Practices for Ocean CO_2 Measurements*. Pices special publication 3, North Pacific Marine Organization, Sidney, Canada, 191 pp.

Field, A. 2007. *Discovering Statistics Using SPSS*, vol. second. SAGE Publications Ltd, London, UK, 816 pp.

Gibson, J. A. E. & Trull, T. W. 1999. Annual cycle of fCO2 under sea-ice and in open water in Prydz Bay, East Antarctica. *Mar. Chem.* 66:187–200.

Grasshoff, K., Ehrhardt, M. & Kremling, K. 1983. *Methods of Seawater Analysis*. Wiley VCH, Weinheim, Germany, 447 pp.

Holm-Hansen, O., Lorenzen, C. J., Homes, R. W. & Strickland, J. D. H. 1965. Fluorometric determination of chlorophyll. *J. Cons. Int. Explor. Mer* 30:3–15.

Hoppema, M. & Goeyens, L. 1999. Redfield behavior of carbon, nitrogen, and phosphorus depletions in Antarctic surface water. *Limnol. Oceanogr.* 44:220–4.

Kim, H. C. & Lee, K. 2009. Significant contribution of dissolved organic matter to seawater alkalinity. *Geophys. Res. Lett.* 36:L20603, 5 pp. DOI: 10.1029/2009GL040271.

Lewis, E. & Wallace, D. W. R. 1998. *Program Developed for CO2 System Calculations*. Carbon Dioxide Information Analysis Center, Oak Ridge National Laboratory, U.S. Department of Energy, Oak Ridge, Tennessee.

Meehl, G. A., Stocker, T. F., Collins, W. D., Friedlingstein, P., Gaye, A. T., Gregory, J. M., Kitoh, A. et al. 2007. Global climate projections. *In* Solomon, S., Qin, D., Manning, M., Chen, Z., Marquis, M., Averyt, K. B., Tignor, M. & Miller, H. L. [Eds.] *Climate Change 2007: The Physical Science Basis. Contribution of Working Group I to the Fourth Assesment Report of the Intergovernmental Panel on Climate Change*. Cambridge University Press, Cambridge, UK and New York, NY, pp. 747–845.

Mehrbach, C., Culberson, C. H., Hawley, J. E. & Pytkowicz, R. M. 1973. Measurement of the apparent dissociation constants of carbonic acid in seawater at atmospheric pressure. *Limnol. Oceanogr.* 18:897–907.

Milligan, A. J., Varela, D. E., Brzezinski, M. A. & Morel, F. M. M. 2004. Dynamics of silicon metabolism and silicon isotopic discrimination in a marine diatom as a function of pCO_2. *Limnol. Oceanogr.* 49:322–9.

Mitchell, B. G., Brody, E. A., Holm-Hansen, O., McClain, C. & Bishop, J. 1991. Light limitation of phytoplankton biomass and macronutrient utilization in the Southern Ocean. *Limnol. Oceanogr.* 36:1662–77.

Moro, I., Paccagnella, R., Barbante, C. & Andreoli, C. 2000. Microalgal communities of the sea ice, ice-covered and ice-free waters of Wood Bay (Ross Sea, Antarctica) during the austral summer 1993-94. *Marine Ecology* 21:233–45.

van de Poll, W. H., Vrieling, E. G. & Gieskes, W. W. C. 1999. Location and expression of frustulins in the pennate diatoms *Cylindrotheca fusiformis*, *Navicula pelliculosa*, and *Navicula salinarum* (Bacillariophyceae). *J. Phycol.* 35:1044–53.

Rampen, S. W., Schouten, S., Schefuss, E. & Damste, J. S. S. 2009. Impact of temperature on long chain diol and mid-chain hydroxy methyl alkanoate composition in *Proboscia* diatoms: results from culture and field studies. *Org. Geochem.* 40:1124–31.

Rampen, S. W., Schouten, S., Wakeham, S. G. & Damste, J. S. S. 2007. Seasonal and spatial variation in the sources and fluxes of long chain diols and mid-chain hydroxy methyl alkanoates in the Arabian Sea. *Org. Geochem.* 38:165–79.

Secher, W. D. & McAvoy, D. C. 2007. *Mineql+ Chemical Equilibrium Modelling System, Version 4.6.1*. Environmental Research software, Hallowell Maine, Maine.

Sweeney, C. 2003. The annual cycle of surface water CO_2 and O_2 in the Ross Sea: a model for gas exchange on the continental shelves of Antarctica. *Antarct. Res. Series* 78:295–312.

Takahashi, T., Sutherland, S. C., Wanninkhof, R., Sweeney, C., Feely, R. A., Chipman, D. W., Hales, B. et al. 2009. Climatological mean and decadal change in surface ocean pCO_2, and net sea-air CO_2 flux over the global oceans. *Deep Sea Res. Part II-Top. Stud. Oceanogr.* 56:554–77.

Timmermans, K. R., Davey, M. S., van der Wagt, B., Snoek, J., Geider, R. J., Veldhuis, M. J. W., Gerringa, L. J. A. & de Baar, H. J. W. 2001. Co-limitation by iron and light of *Chaetoceros brevis*, *C. dichaeta* and *C. calcitrans* (Bacillariophyceae). *Mar. Ecol. Prog. Ser.* 217:287–97.

Verardo, D. J., Froelich, P. N. & McIntyre, A. 1990. Determination of organic carbon and nitrogen in marine sediments using the Carlo-Erba-Na-1500 Analyzer. *Deep-Sea Res. Part A-Oceanogr. Res. Pap.* 37:157–65.

Vrieling, E. G., Sun, Q., Beelen, T. P. M., Hazelaar, S., Gieskes, W. W. C., van Santen, R. A. & Sommerdijk, N. A. J. M. 2005. Controlled silica synthesis inspired by diatom silicon biomineralization. *J. Nanosci. Nanotechnol.* 5:1–11.

Weiss, R. F. 1974. Carbon dioxide in water and Seawater: the solubility of a non-ideal gas. *Mar. Chem.* 2:203–15.

Supplementary Material

The following supplementary material is available for this article:

Figure S1. The cell abundance of *Proboscia alata* in the six different treatments.

Figure S2. The relationship between the expected A_T and the measured A_T, both in $\mu mol \cdot kg^{-1}$.

Figure S3. The relationship between the ΔA_T (measured – expected A_T) ($\mu mol \cdot kg^{-1}$) and the [DOC] ($\mu mol \cdot l^{-1}$).

Figure S4. The silicate speciation in the 6 different treatments as calculated from the pH, DIC and silicate data.

This material is available as part of the online article.

Please note: Wiley-Blackwell are not responsible for the content or functionality of any supporting materials supplied by the authors. Any queries (other than missing material) should be directed to the corresponding author for the article.